10.1590/s1982-21702018000400033

ARTICLE

STOCHASTIC MODEL OF THE BRAZILIAN GPS NETWORK COORDINATES TIME SERIES

Modelo Estocástico das Series de Coordenadas GPS da Rede Brasileira de Monitoramento Continuo

Christian Gonzalo Pilapanta Amagua[1,2] - ORCID: 0000-0003-1155-7173

Claudia Pereira Krueger[1] - ORCID: 0000-0002-4839-1317

Alfonso Rodrigo Tierra Criollo[2] - ORCID: 0000-0002-2885-0088

[1] Universidade Federal do Paraná, Setor de Ciências da Terra, Departamento de Geomática, Programa de Pós-Graduação em Ciências Geodésicas, Curitiba, Paraná, Brasil.
E-mail: cgpilapanta@gmail.com, ckrueger@ufpr.br

[2] Universidad de las Fuerzas Armadas - ESPE, Centro Geoespacial, Sangolquí, Ecuador.
E-mail: artierra@espe.edu.ec

Received in January 30th, 2018
Accepted in August 17th, 2018

Abstract:

It is well known that daily estimates of GPS coordinates are highly temporally correlated and that the knowledge and understanding of this correlation allows to establish more realistic uncertainties of the parameters estimated from the data. Despite this, there are currently no studies related to the analysis and calculation of the noise sources in geodetic time series in Brazil. In this context, this paper focuses on the investigation of the stochastic properties of a total of 486 coordinates time series from 159 GPS stations belonging to the Brazilian Network for Continuous Monitoring of GNSS (RBMC) using the maximum likelihood estimation approach. To reliably describe the GPS time series, we evaluate 4 possible stochastic models as models of each time series: 3 models with integer spectral indices (white noise, flicker plus white noise and random-walk plus white noise model) and 1 with fractional spectral index (fractional power-law plus white noise). By comparing the calculated noise content values for each model, it is possible to demonstrate a stepwise increase of the noise content, being the combination of a fractional power-law process and white noise process, the model with smaller values and the combination of random walk process with white noise process, the model with greater values. The analysis of the spatial distribution of the noise values of the processes allow demonstrate that the GPS sites with the highest accumulated noise values, coincide with sites located in coastal zones and river basins and that their stochastic properties can be aliased by the occurrence of different physical signals typical of this type of zones, as the case of the hydrological loading effect.

Keywords: Time series analysis; Stochastic model, Power-Law noise model

How to cite this article: AMAGUA, C. G. P. *et al*. Stochastic Model of the Brazilian GPS Network Coordinates Time Series. *Bulletin of Geodetic Sciences*, Vol. 24 (4): 545-563, Oct-Dec, 2018.

Resumo:

É bem conhecido que as estimativas diárias das coordenadas GPS se encontram fortemente correlacionadas temporalmente. O conhecimento e compreensão desta correlação, permite estabelecer em princípio, incertezas mais realistas dos parâmetros estimados a partir dos dados. Apesar disso, atualmente não existem estudos relacionados à análise e cálculo dos sinais de ruído em série temporal de coordenadas GPS no Brasil. Neste sentido, a presente pesquisa visa estudar as propriedades estocásticas de um total de 486 séries temporais compostas de 10 anos de observações de 159 estações GPS pertencentes à Rede Brasileira de Monitoramento Contínuo de GNSS (RBMC) através da implementação do estimador de máxima verossimilhança. Para descrever de forma adequada as series temporais avaliadas, foram avaliados 4 possíveis modelos estocásticos como modelos de cada série temporal, sendo: 3 modelos com índices espectrais inteiros e 1 com índice espectral fracionário. A comparação das variâncias dos sinais de ruído dos modelos permitiu demonstrar um aumento gradual dos mesmos. Sendo que, a combinação de um processo de lei de potências fracionário e de um processo de ruído branco forneceu o modelo com as menores variâncias, e, a combinação de um processo de random-walk com um processo de ruído branco gerou o modelo com as maiores variâncias. A análise da distribuição espacial dos valores de ruído dos processos permitiu demonstrar que as localizações dos pontos GPS com maiores variâncias acumuladas de ruído, coincidem com os pontos localizados em zonas costeiras e bacias hidrográficas e que suas propriedades estocásticas podem ser afetadas pela ocorrência de diferentes sinais físicos típicos deste tipo de zonas, como no caso do efeito de carga hidrológica.

Palavras-chave: Análise de series de tempo; modelo estocástico; lei de potências

1. Introduction

It is well known that the noise in continuous GPS observations, as with many geophysical phenomena, can be described as a power-law process (Mandelbrot and Van Ness, 1968; Agnew, 1992). That is, a one-dimensional stochastic process whose time-domain behaviour is such that its power spectrum has the form

$$P(f) = P_0 \left(\frac{f}{f_0} \right)^k \tag{1}$$

where P_0 and f_0 are normalizing constants, f is spatial or temporal frequency and k is the spectral index. In most cases, the spectral index k lies within the range $-3 < k < 1$ and it can be subdivided into "fractional Brownian motions" with $-3 < k < -1$ and "fractional Gaussian noise" with $-1 < k < 1$. Special cases of these processes also include the classical Brownian motion (called "random-walk noise") with $k = -2$, the "flicker noise" process with $k = -1$ and the uncorrelated "white noise" process with $k = 0$.

The importance of knowing and understanding the noise content of GPS data is because it allows establishing more realistic uncertainties of the parameters estimated from them. Johnson & Agnew (1995), for instance, demonstrated that neglecting the effect of long-range time-

dependent correlations noise, makes the uncertainty in the estimated velocities much too small, and if the correlated and independent noise sources have a similar magnitude, the expected improvement in uncertainty from having more measurements is minimum. Zhang et al. (1997), in turn, showed that if the noise of data is purely white, it generates an underestimation of site rate uncertainties 3 or 5 times greater than when using a white plus flicker noise process, a more suitable stochastic model. Likewise, Langbein and Johnson (1997), found that the correlated nature of random-walk noise can cause time-dependent fluctuations in the time series which could be misinterpreted as tectonic signals if these were not previously eliminated. Finally, Williams (2003), proved that the uncertainties of sites rates could be estimated on the basis of the error model $\varepsilon_x(t_t)$ assumed for the data. This can be expressed as a linear combination of independent unit-variance random variables $\alpha(t_i)$ and temporally correlated random variables $\beta(t_i)$, such that

$$\varepsilon_x(t_i) = a\alpha(t_i) + b_k\beta(t_i) \tag{2}$$

where a and b_k are the variance of white noise and coloured noise (power-law processes other than classical white noise) of spectral index k respectively.

Currently, there are many different methods for assessing the noise content and their elements in time series (Johnson and Agnew, 1995; Langbein and Johnson, 1997; Wdowinski *et al.*, 1997; Zhang *et al.*, 1997; Mao *et al.*, 1999), however, the most robust is the Maximum Likelihood Estimator (MLE) (Bos *et al.*, 2008, 2013; Williams, 2008). It estimates the noise components and the other parameters of the stochastic model, finding the set of values of the model that maximize their likelihood function (Langbein and Johnson, 1997). In general, the MLE can be found the set of values as an explicit function of the observed data, or through global numerical optimization (Bos *et al.*, 2008, 2013). Based on the aforementioned, and because currently there are no studies related to the analysis and calculation of the noise sources in GPS time series in Brazil, this study seeks to establish the basis for the description of GPS time series uncertainties at the national level. In this regard, this paper focuses on the analysis of the stochastic properties of the time series of weekly position estimates for 159 sites of the Brazilian Network for Continuous Monitoring of GPS using the modified MLE algorithm established by Bos *et al.*, (2013). Finally, we examined 4 different possible stochastic models. They are a classic white noise (WN), a flicker plus white noise (FL+WN), a random-walk plus white noise RW+WN) and a fractional power-law noise model.

2. Stochastic model estimation

2.1 Maximum Likelihood Estimator

According to Langbein & Johnson (1997), estimating the noise components and the parameters from the linear function using the maximum likelihood estimator (MLE), requires maximizing the

probability function by adjusting the data covariance. Thus, given a vector of observations x, the likelihood function for a covariance matrix C (which represents the assumed noise in the data) is

$$l(x,C) = \frac{1}{(2\pi)^{N/2}(\det C)^{1/2}} \exp\left(-0,5\hat{v}^T C^{-1}\hat{v}\right) \tag{3}$$

where N is the number of data (epochs), $\det$ is the determinant of a matrix and $\hat{v}$ are the post-fit residuals to the linear function using weighted least squares with the same covariance matrix C. For greater numerical stability and since the maximum is unaffected by monotonic transformation, it is often convenient to work with the logarithm form of (3). In this case, the log-likelihood function is given by

$$\ln\left[l(x,C)\right] = -\frac{1}{2}\left[\ln(\det C) + \hat{v}^T C^{-1}\hat{v} + N\ln(2\pi)\right] \tag{4}$$

According to Williams (2008), sometimes it is also necessary to estimate other parameters of the stochastic model than the noise values (common examples of these are the spectral index k of power-law noise models and the cross-over parameter β in first-order Gauss-Markov noise) (Langbein, 2004). This can be done if we include the parameters as extra dimensions in a general uphill simplex together with the set of noise values, however, this process is not recommended because at most iterations the uphill simplex may choose a new value for one of these parameters and therefore create a new unit covariance matrix. The alternative to this is to split the maximization process into two parts. Initially, we can estimate the noise values for fixed noise model parameters (inner maximization) and after that, we can use an outer maximization to estimate the other parameters. The result of this process is an adequate treatment of the routines that deal with covariance matrices (creation, inversion and determinant estimation) and probably to a more stable process. In this sense, the problem of calculating the noise values is reduced to the correct deduction of the covariance matrix.

2.2 Covariance matrix of stochastic models

The data covariance matrix can usually be represented through the combination of different stochastic models. That is

$$C = \sum_{i=1}^{m} \sigma_i^2 C_{PL} \tag{5}$$

where m represents a total number of stochastic models, C_{PL} are the unit covariance matrices for temporally correlated noise (power law noise with spectral index k) and σ_i^2 the variance of

the stochastic models. For instance, if we take into consideration the 3 main processes cited in section 1 (random-walk noise, flicker noise and classical white noise), the matrix C takes the form

$$C = \sigma_{WN}^2 I + \sigma_{RW}^2 C_{RW} + \sigma_{FL}^2 C_{FL} \tag{6}$$

where I is the $N \times N$ identity matrix (unit covariance matrix for white noise – no cross-correlation) and C_{RW} and C_{FL} are the unit covariance matrices for random-walk and flicker noise. It is important to note that if the covariance matrix consists of only one noise source, then it takes the form

$$C = \sigma^2 C_{PL} \tag{7}$$

and therefore, the log-likelihood function (4) can be re-written as

$$\ln\left[l\left(x,\sigma\right)\right] = -\frac{1}{2}\left[2\,\mathrm{N}\ln\left(\sigma\right) + \ln\left(\det C_{PL}\right) + \frac{\hat{v}^T C_{PL}{}^{-1}\hat{v}}{\sigma^2} + N\ln\left(2\pi\right)\right] \tag{8}$$

In this case, the residuals $\hat{v}$ and the estimated parameters can be considered invariant to a scale change in the covariance matrix C (least squares adjustment) (Williams, 2008) and therefore, it is possible to differentiate (7) respect to σ and obtain its true value explicitly by

$$\sigma = \sqrt{\frac{\hat{v}^T C_{PL}{}^{-1}\hat{v}}{N}} \tag{9}$$

Meanwhile, if the covariance matrix C depends on more than one noise source, it is necessary to transform the noise variances to a new common that allows an only one-dimensional numerical maximization (Bos *et al.*, 2008; Williams, 2008). For instance, if we have two noise variances σ_1 and σ_2 it is possible to transform these to two alternative variables namely an angle ϕ and a common variance σ (driving noise) such that

$$\begin{aligned} \sigma_1 &= \sigma\cos\phi \\ \sigma_2 &= \sigma\sin\phi \end{aligned} \tag{10}$$

So, in this case, we can compute a unit covariance matrix C by

$$C = \sigma^2 \left(\cos^2 \phi C_{PL-1} + \sin^2 \phi C_{PL-2} \right) \tag{11}$$

where C_{PL-1} and C_{PL-2} are the unit covariance matrices for temporally correlated noises with variances σ_1 and σ_2 respectively. A generalization of this model was obtained by Bos et al. (2008), who redefined C for $N+1$ noise models as

$$C = \sigma^2 \left(\phi_1 C_{PL-1} + (1-\phi_1)\phi_2 C_{PL-2} + (1-\phi_1)(1-\phi_2)\phi_3 C_{PL-3} + ... + (1-\phi_1)(1-\phi_2)...\phi_N C_{PL-N+1} \right) \tag{12}$$

In this case, all angles ϕ vary only between 0 and 1. The result of this new model is a Toeplitz covariance matrix C, where only the first column γ_i determines all its properties (descending diagonal from left to right is constant). In this regard, for instance, the first column γ_i of the covariance matrix C for any power-law noise model is (Bos *et al.*, 2008):

$$\gamma_i = \frac{\Gamma(d+i)\Gamma(1-2d)}{\Gamma(d)\Gamma(1+i-d)\Gamma(1-d)} \tag{13}$$

where d is $-1/2$ time the spectral index k. Another important and classical noise model used in the analysis of geodetic times series and which can be determined from (12), is the Generalized Gauss Markov noise. For this, Langbein (2004) modified the classical first-order Gauss Markov model and include the spectral index d in the equation to create a power-law noise with a slope of $2d$ in the power density spectrum, which flattens to white noise at the very low and very high frequencies (Bos *et al.*, 2008). The new equation for the autocovariance vector γ_i is

$$\gamma_i = \frac{\Gamma(d+i)\Gamma(1-\phi)}{\Gamma(d)\Gamma(1-i)} 2F_1\left(d, d+i, 1+i, (1-\phi)^2\right) \tag{14}$$

A more robust description of the covariance matrices for each stochastic model using in geodetic studies can be found in Williams (2003), Bos et al. (2008), Williams (2008) and Langbein & Johnson (1997). For the present study, we used the research of Williams (2003) as the standard research to follow.

2.3 Bayesian Information Criterion

Once the parameter values of the stochastic model have been obtained, it is important to compare the Maximum Likelihood values considering the complexities of the different models (number of estimated parameters both in the linear and the stochastic model) and determine which model is the best adapted to the GPS data. For this, one of the most used tests is the Bayesian Information Criteria (BIC), which is defined as

$$BIC = -2MLE + p\ln\left(N\right) \tag{15}$$

where MLE is a maximum likelihood estimation value, p is the number of estimated parameters, and N is the number of data. The best model will be the one with the lowest BIC value.

Other criteria used to evaluate the quality of the chosen noise models are the Akaike Information Criteria (AIC), the Deviance Information Criterion (DIC) and the Focused Information Criterion (FIC). A detailed analysis of the selection criteria can be found in Kadane and Lazar (2004).

3. Data and Methods

In this study, we analyze the time series of weekly position estimates for 159 sites of the Brazilian Network for Continuous Monitoring of GNSS, RBMC, obtained in the last 10 years (2007 – 2017). The lengths of the time series range between 1 and 10 years (To see the individual time span of the time series for all GPS station used in the experiments see http://www.sirgas.org/es/sirgas-con-network/stations/station-list/#). The station coordinates were calculated by the data processing centres of the Geocentric Reference System for the Americas (SIRGAS) and available at the ftp://ftp.sirgas.org/pub/gps/SIRGAS. The details concerning processing of GNSS observations can be found in Sánchez *et al.*, (2015) and the RBMC official site https://ww2.ibge.gov.br/home/geociencias/geodesia/rbmc/analise.shtm.

3.1 Maximum Likelihood Estimation

Once the residuals have been obtained, we apply the MLE equations to these (section 2.1) to evaluate their stochastic properties. In this study, we evaluate 4 possible stochastic models. They are 3 classical models with integer spectral indices (WN – White noise; FL + WN – flicker plus white noise and RW + WN – random-walk plus white noise model) and 1 model with fractional spectral index (PF + WN – Fractional power-law plus white noise). The respective unit covariance C for each of temporally correlated noises (WN, FL, RW noises) was obtained using (13) and included in the estimation as fixed parameters (inner estimation) together with other parameters of interest such as variance and phase of seasonal signals and offsets. Maximum likelihood estimates of the values of noise sources for all 159 RBMC time series are presented in Appendix 5.1.

4. Results and Discussion

Figure 1 and Table 1 provide the distribution of the optimal noise models (based on BIC criteria) for the RBMC data. The results show that roughly 70% to 80% of the best noise models are a combination of flicker noise plus white noise. The combination of random-walk plus white noise characterizes between 5% and 16% of the time series and the remaining 5% of the time series are split between the classical white noise model and a fractional power-law noise process.

Table 1: Distribution of noise models for the RBMC data

ORD	STOCHASTIC MODEL	EAST		NORTH		UP	
		TOTAL	%	TOTAL	%	TOTAL	%
1	White Noise	17	11	14	9	21	13
2	Flicker Noise + White Noise	110	69	127	80	115	72
3	Random-Walk Noise + White Noise	26	16	8	5	17	11
4	Fractional Power-Law noise + White Noise	6	4	10	6	6	4

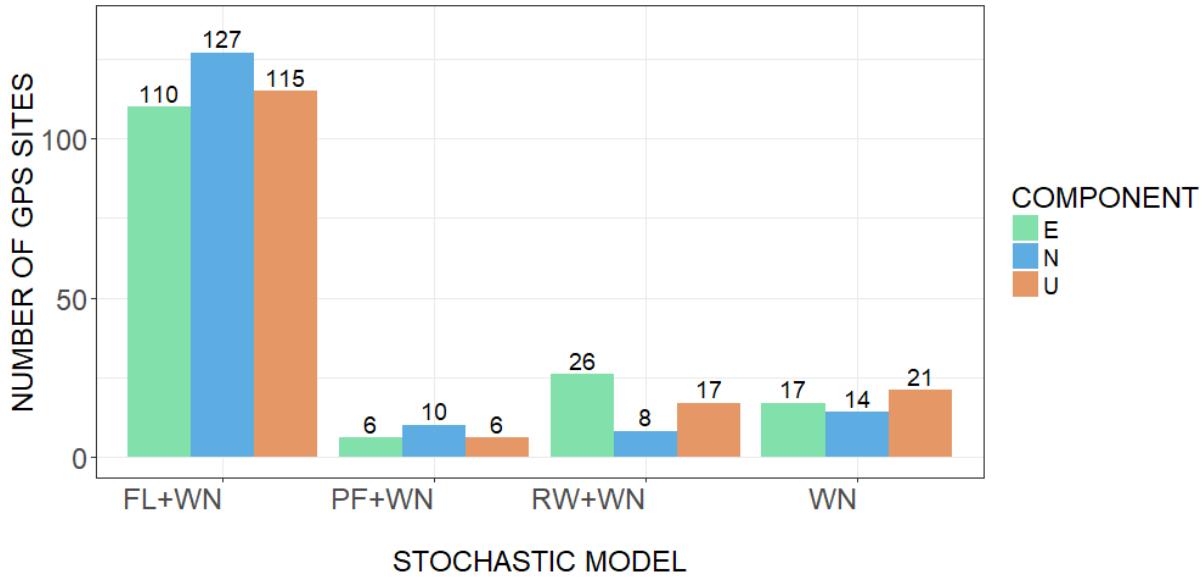

Figure 1: Distribution of noise models for the RBMC data

An important aspect to consider is that most of the existing studies only use a power-law noise process to calculate the stochastic model of the time series (Bos et al., 2013; Williams, 2015; Klos et al., 2016; Klos, Bogusz and Moreaux, 2017). In this regard, if we apply a fractional power-law model to all RBMC time series, the spectral index k of the sites lies between -1 or 1 (fractional Gaussian noise) and, in most cases, this tends to be -1 (Figure 2). Initially, this behaviour agrees with the results presented in Table 2 (Flicker nose with $k=-1$), however, the fractional power-law model is not able to detect the presence of random-walk noise in the time series and therefore, it has a limitation in the modelling compared to the approach used in this study.

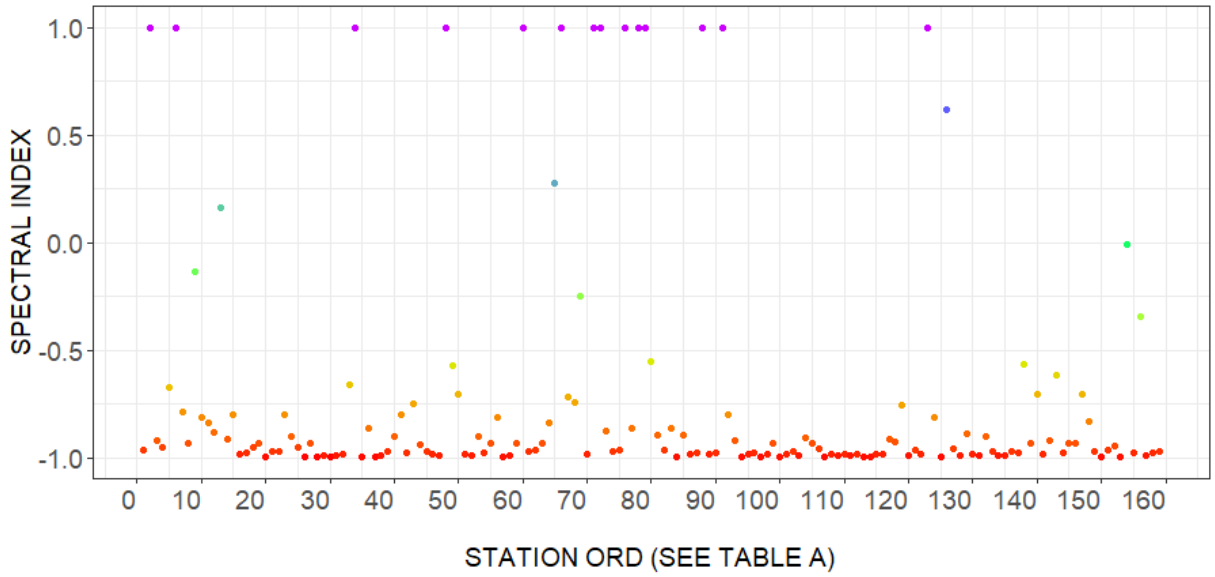

Figure 2: Spatial distribution of noise values of GPS sites

A summary of the noise magnitudes for each solution is provided in Table 2. In principle, it is possible to see that the stochastic model with the lowest magnitudes of noise is the fractional power-law plus white noise model (PF + WN), whose accumulated noise variances ($\Sigma\sigma = \sigma_{PL} + \sigma_{WN}$) are in order of 0,15 mm for the horizontal components and 3 mm for the vertical component. (The symbol "-" indicates that the estimation made did not obtain a noise value for the specified model). It is important to note, the fact that the mean variance of the white noise in this model is almost zero and therefore, it does not represent even one percent of the total accumulated noise value. The next models are the classical white noise model with accumulated noise variance in order of 0,7 mm for horizontal components and 2 mm for vertical component, the Flicker noise plus white noise, with accumulated noise variances of 3 mm for horizontal components and 10 mm for the vertical component and the Random-walk plus white noise with accumulated noise variances in order of 6 mm for horizontal components and 15 mm for vertical component. An interesting detail to emphasize is the growing tendency of the accumulated noise variances between combined models (white noise plus power-law noise) (i.e. the noise grows by a factor of 3). For instance, the variance of PF + WN model is 3 times lower than the variance of FW + WN model, and this is 3 times lower than the variance of RW + WN. The same applies to the components of the sites. In this case, the horizontal components are also less noisy than the vertical component by a factor of 3, which coincides with results obtained in other studies (Zhang *et al.*, 1997; Mao *et al.*, 1999; Langbein, 2004)

Table 2: Noise values and selected stochastic models of GPS sites

ORD	PARAMETER	MODEL	EAST			NORTH			UP		
			σ_{PL} (mm/yr$^{k/4}$)	σ_{WN} (mm)	$\Sigma\sigma$ (mm)	σ_{PL} (mm/yr$^{k/4}$)	σ_{WN} (mm)	$\Sigma\sigma$ (mm)	σ_{PL} (mm/yr$^{k/4}$)	σ_{WN} (mm)	$\Sigma\sigma$ (mm)
1	Mean	WN	-	0,67	0,67	-	0,75	0,75	-	2,12	2,12
		FL + WN	2,80	0,37	3,17	3,16	0,38	3,55	8,23	1,09	9,32
		RW + WN	5,98	0,61	6,59	5,56	0,72	6,27	14,94	1,69	16,63
		PF + WN	0,12	0,01	0,13	0,14	0,01	0,15	3,76	0,01	3,77
2	Minimum	WN	-	0,15	0,15	-	0,14	0,14	-	0,85	0,85
		FL + WN	1,65	0,05	1,70	1,63	0,02	1,65	5,24	0,26	5,50
		RW + WN	4,58	0,35	4,93	4,29	0,41	4,70	10,36	0,45	10,81
		PF + WN	0,06	0,01	0,07	0,11	0,01	0,12	0,38	0,01	0,39
3	Maximum	WN	-	1,16	1,16	-	1,27	1,27	-	4,03	4,03
		FL + WN	4,27	0,78	5,05	4,72	0,86	5,59	14,52	2,93	17,46
		RW + WN	8,60	0,99	9,59	7,85	1,03	8,88	20,75	3,53	24,28
		PF + WN	0,22	0,01	0,23	0,20	0,01	0,21	8,21	0,03	8,24

* WN: White noise; FL: Flicker noise; RW: Random-walk; PF: Power-Law (fractional) noise; PL: Power-Law noise

On the other hand, it is important to note the high magnitudes of the noise of the RW + WN model when compared to the others. In this regard, Table 3 shows the 10 sites with the highest accumulated noise values. The clear majority of them are just an RW + WN process.

Table 3: Sites with the highest accumulated noise values

ORD	SITE	MODEL	$\Sigma\sigma$ (mm)	SITE	MODEL	$\Sigma\sigma$ (mm)	SITE	MODEL	$\Sigma\sigma$ (mm)
1	CRAT	RW+WN	9,36	UBA1	RW+WN	8,67	NAUS	RW+WN	20,75
2	CEFT	RW+WN	8,51	CUIB	RW+WN	6,75	AMTE	FL+WN	20,14
3	VARG	RW+WN	8,45	RECF	FL+WN	6,69	BATF	RW+WN	17,10
4	UBA1	RW+WN	8,01	SCAQ	RW+WN	6,23	AMUA	FL+WN	18,83
5	BRAZ	RW+WN	7,34	SJSP	RW+WN	6,00	BRAZ	RW+WN	17,58
6	BATF	RW+WN	7,33	SAGA	FL+WN	5,57	ITAM	FL+WN	17,39
7	SSA1	RW+WN	7,04	RSAL	RW+WN	5,41	SAGA	FL+WN	14,16
8	CEEU	RW+WN	6,99	MSCG	FL+WN	4,91	AMPR	FL+WN	15,55
9	RNMO	RW+WN	6,92	AMTE	FL+WN	4,87	ROGM	FL+WN	14,20
10	CUIB	RW+WN	6,79	POLI	FL+WN	4,72	COAM	FL+WN	14,39

* WN: White noise; FL: Flicker noise; RW: Random-walk; PL: Power-Law noise

According to Langbein and Johnson, (1997), this marked variability of the RW+WN noise model, is often due to the incidence of two principal processes: the precision of the instrument and the motion of the geodetic monument. To analyze this precept, Figure 3 illustrates the location of all GPS sites together with the spatial distribution of the vertical accumulated noise.

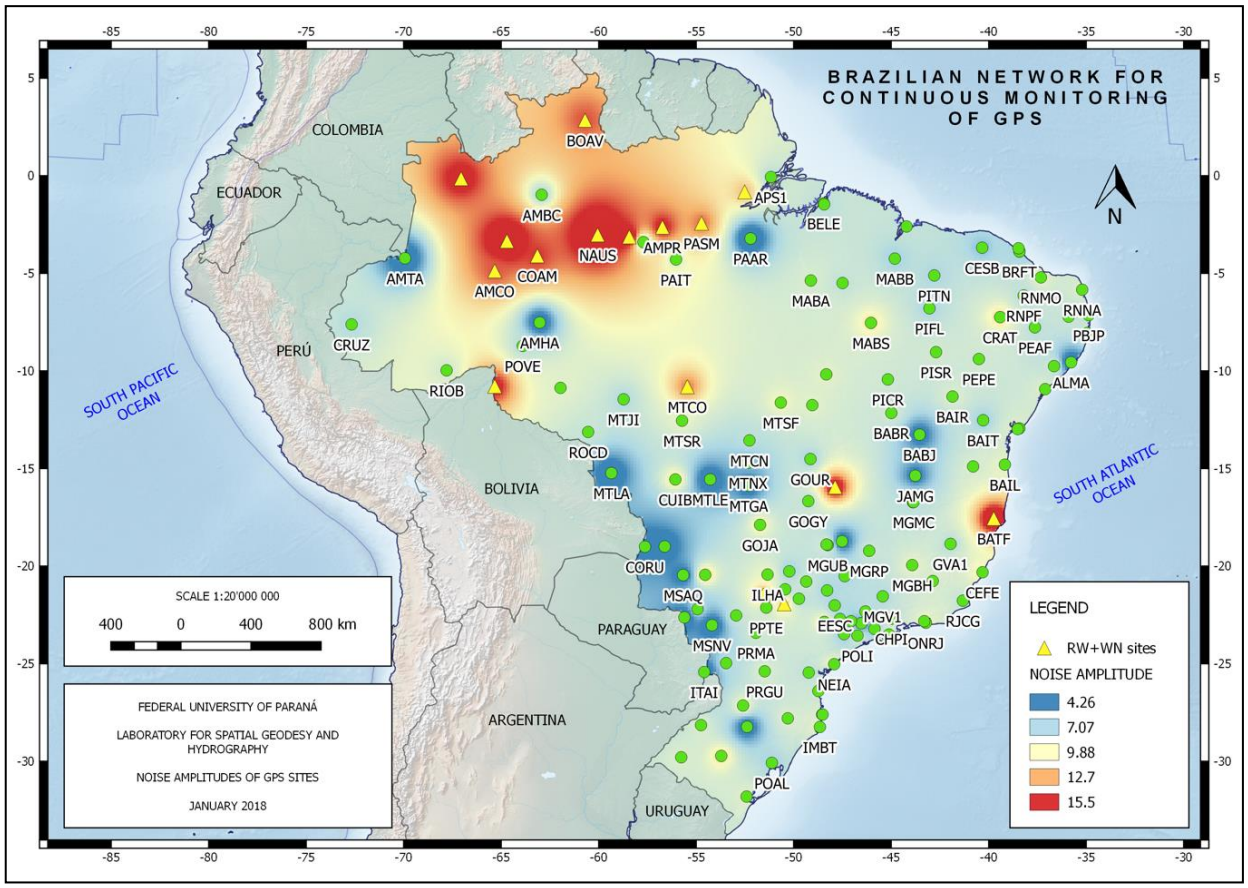

Figure 3: Spatial distribution of noise values of GPS sites. Up component

As can be seen from the Figure 3, it is evident that most GPS sites, whose stochastic model is an RW + WN process, coincide with sites located in coastal zones and river basins. Initially, it may imply that the behaviour of the data of these stations is aliased by the prevalence of different physical signals typical of this type of zones, such as the hydrological, non-tidal oceanic loading or atmospheric pressure loading. A particular example of a GPS site whose motion is aliased by external physical effects is the NAUS station, whose vertical displacements can vary around 7 cm (variance of seasonal signal) (Figure 4).

It is interesting to see that in the present research, the Manaus station is precisely the station with the highest level of noise. It suggests that the claim that the high variances of RW + WN processes are produced by the motion of the site is correct, however, there is not enough evidence to ensure this. Finally, a detailed description of the variances of the noises for each station is presented in appendix 5.1.

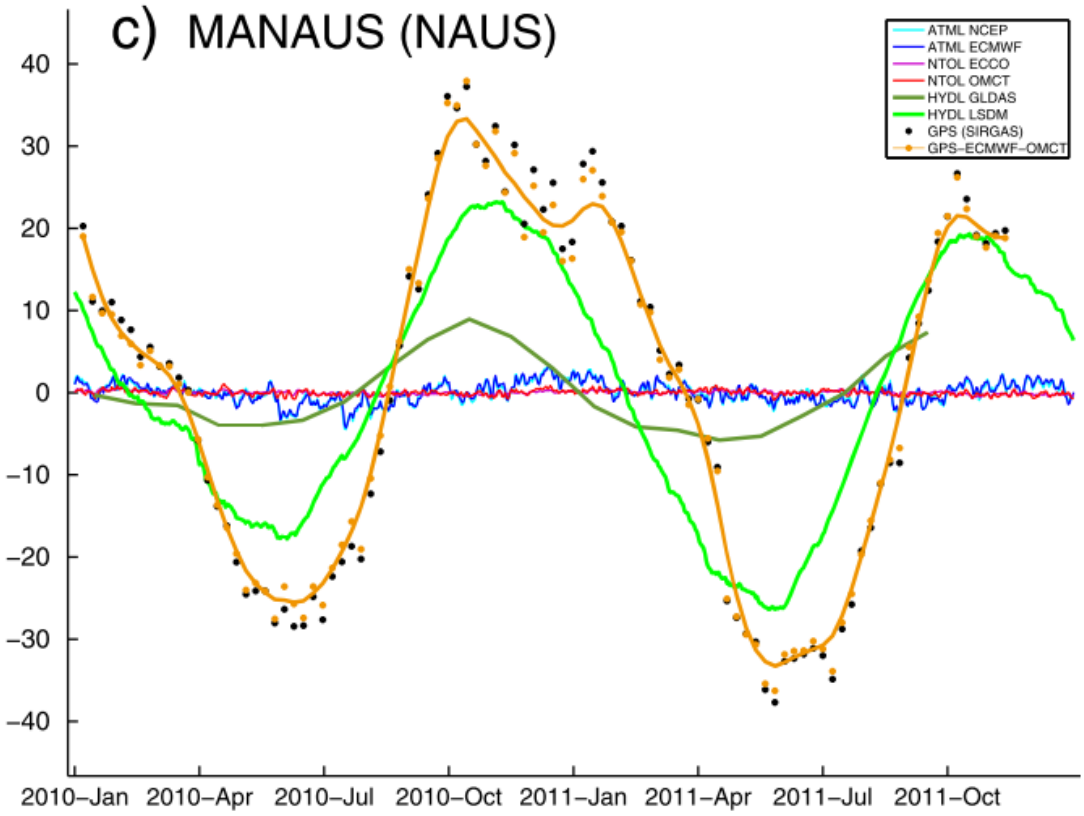

Figure 4: Vertical displacement (mm) of MANAUS site together with the hydrological (HYDL), non-tidal ocean loading (NTOL) and atmospheric pressure loading contributions (ATML)

Source: Dill and Dobslaw (2013)

4. Conclusion

We have analyzed the stochastic properties of GPS position time series of the 159 sites of the Brazilian Network for Continuous Monitoring of GNSS, RBMC, obtained in the last 10 years (2007 – 2017) and determine that more than 90% of these stations have as stochastic model a linear combination of white noise process and either a flicker noise or random-walk noise process. Comparison of the variances of models allows demonstrating a stepwise increase of the noise variances, being the combination of a fractional power-law process and white noise process, the model with smaller variances and the combination of random walk process with white noise process, the model with greater variances. The analysis of the spatial distribution of the noise variances of the processes allow demonstrate that the GPS sites with the highest accumulated noise variances, coincide with sites located in coastal zones and river basins and that their stochastic properties can be aliased by the occurrence of different physical signals typical of this type of zones, though we cannot prove that this is the case.

Acknowledgement

The authors would like to thank the Coordination for the Improvement of Higher Education Personnel (CAPES) for their financial support and SIRGAS and IBGE for making publicly available the position time series used in this study.

References

Agnew, D. C. (1992). The Time-Domain behavior of Power-Law noises. *Geophysical Research Letters*, 19(4), pp. 333–336.

Bos, M. S. et al. (2008). Fast error analysis of continuous GPS observations. *Journal of Geodesy*. doi: 10.1007/s00190-007-0165-x.

Bos, M. S. et al. (2013). Fast error analysis of continuous GNSS observations with missing data. *Journal of Geodesy*, 87, pp. 351–360. doi: 10.1007/s00190-012-0605-0.

Dill, R. and Dobslaw, H. (2013). Numerical simulations of global-scale high-resolution hydrological crustal deformations. *Journal of Geophysical Research: Solid Earth*, 118(9), pp. 5008–5017. doi: 10.1002/jgrb.50353.

Johnson, H. O. and Agnew, D. C. (1995). Monument motion and measurements of crustal velocities. *Geophysical Research Letters*, 22(21), pp. 2905–2908. doi: 10.1029/95GL02661.

Kadane, J. B. and Lazar, N. A. (2004). Methods and Critera for Model Selection. *Journal of the American Statistical Association*, 99(465), pp. 279–290. doi: 10.1198/016214504000000269.

Klos, A. et al. (2016). Noise analysis of continuous GPS time series of selected EPN stations to investigate variations in stability of monument types. In *International Association of Geodesy Symposia*. doi: 10.1007/1345_2015_62.

Klos, A., Bogusz, J. and Moreaux, G. (2017). Stochastic models in the DORIS position time series: estimates for IDS contribution to ITRF2014. *Journal of Geodesy*, pp. 1–21. doi: 10.1007/s00190-017-1092-0.

Langbein, J. (2004). Noise in two-color electronic distance meter measurements revisited. *Journal of Geophysical Research B: Solid Earth*. doi: 10.1029/2003JB002819.

Langbein, J. and Bock, Y. (2004). High-rate real-time GPS network at Parkfield: Utility for detecting fault slip and seismic displacements. *Geophysical Research Letters*, 31(15), pp. 2–5. doi: 10.1029/2003GL019408.

Langbein, J. and Johnson, H. (1997). Correlated errors in geodetic time series: Implications for time-dependent deformation. *Journal of Geophysical Research*, 102(10), pp. 591–603. doi: 10.1029/96JB02945.

Mandelbrot, B. B. and Van Ness, J. W. (1968). Fractional Brownian Motions, Fractional Noises and Applications. *SIAM Review*, 10(4), pp. 422–437. doi: 10.1137/1010093.

Mao, A. et al. (1999). Noise in GPS coordinate time series. *Journal of Geophysical Research*, 104(B2), pp. 2797–2816. doi: 10.1029/1998JB900033.

Montecino, H. D., de Freitas, S. R. C., Báez, J. C., & Ferreira, V. G. (2017). Effects on Chilean Vertical Reference Frame due to the Maule Earthquake co-seismic and post-seismic effects. *Journal of Geodynamics*, 112, pp.22–30.

Sánchez, L. et al. (2015). SIRGAS Core Network Stability. *International Association of Geodesy Symposia*, 143, pp. 183–191. doi: 10.1007/1345_2015_143.

Wdowinski, S. et al. (1997). Southern California permanent GPS geodetic array: Spatial filtering of daily positions for estimating coseismic and postseismic displacements induced by the 1992 Landers earthquake. *Journal of Geophysical Research: Solid Earth*, 102(B8), pp. 18057–18070. doi: 10.1029/97JB01378.

Williams, S. (2003). The effect of coloured noise on the uncertainties of rates estimated from geodetic time series. *Journal of Geodesy*, 76, pp. 483–494. doi: 10.1007/s00190-002-0283-4.

Williams, S. (2015). Description of GPS uncertainties within the Long Term Study on Anomalous Time-Dependent Subsidence.

Williams, S. D. P. (2003). Offsets in Global Positioning System time series. *Journal of Geophysical Research*, 108. doi: 10.1029/2002JB002156.

Williams, S. D. P. (2008). CATS: GPS coordinate time series analysis software. *GPS Solutions*, 2, pp. 147–153. doi: 10.1007/s10291-007-0086-4.

Zhang, J. et al. (1997). Southern California Permanent GPS Geodetic Array. Error Analysis of Daily Position Estimates and Sites Velocities. *Journal of Geophysical Research*, 102(B8), pp. 18035–18055. doi: 10.1029/97JB01380.

Appendix and attachments

1. Noise variances of selected stochastic models

Table A: Noise variances and selected stochastic models of GPS sites

Continue

ORD	SITE	EAST			NORTH			UP		
		MODEL	σ_{PL} (mm/yr$^{-k/4}$)	σ_{WN} (mm)	MODEL	σ_{PL} (mm/yr$^{-k/4}$)	σ_{WN} (mm)	MODEL	σ_{PL} (mm/yr$^{-k/4}$)	σ_{WN} (mm)
1	ALAR	FL+WN	3,32	-[1]	FL+WN	3,57	-	FL+WN	8,88	-
2	ALMA	PF+WN	0,06	-	PF+WN	0,15	-	WN	-	0,85
3	AMBC	FL+WN	1,98	-	FL+WN	1,68	0,26	FL+WN	7,37	-
4	AMCO	FL+WN	2,48	-	FL+WN	2,97	-	RW+WN	12,79	1,79
5	AMHA	FL+WN	2,22	0,51	WN	-	0,83	WN	-	2,38
6	AMHU	PF+WN	0,22	-	PF+WN	0,18	0,01	WN	-	2,38
7	AMMU	FL+WN	2,10	-	FL+WN	2,04	-	FL+WN	6,49	-
8	AMPR	FL+WN	2,07	-	FL+WN	2,66	-	RW+WN	15,55	1,15
9	AMTA	WN	-	0,76	FL+WN	2,35	-	WN	-	2,24
10	AMTE	FL+WN	2,56	0,57	RW+WN	4,29	0,58	RW+WN	20,14	1,09
11	AMUA	FL+WN	2,21	0,05	FL+WN	2,03	-	RW+WN	18,83	0,45
12	APLJ	FL+WN	1,85	0,17	FL+WN	2,53	-	RW+WN	10,36	1,50
13	APS1	WN	-	0,62	WN	-	0,64	FL+WN	7,81	-
14	APSA	FL+WN	2,41	0,25	FL+WN	3,11	-	FL+WN	7,73	0,97
15	BABJ	FL+WN	1,65	-	FL+WN	2,30	-	WN	-	2,37
16	BABR	FL+WN	3,04	-	FL+WN	3,24	0,21	FL+WN	8,64	-
17	BAIL	FL+WN	2,76	-	FL+WN	2,75	0,42	FL+WN	9,13	0,26
18	BAIR	FL+WN	3,05	-	FL+WN	3,38	-	FL+WN	8,94	-
19	BAIT	FL+WN	2,29	-	FL+WN	2,08	0,27	FL+WN	6,73	-
20	BATF	RW+WN	6,34	0,99	FL+WN	3,83	-	RW+WN	17,10	3,53
21	BAVC	FL+WN	3,14	-	FL+WN	3,67	-	FL+WN	8,69	-
22	BELE	FL+WN	2,94	-	FL+WN	3,63	0,21	FL+WN	8,56	-
23	BEPA	FL+WN	2,33	0,26	FL+WN	2,90	-	FL+WN	7,14	-
24	BOAV	FL+WN	2,54	0,29	FL+WN	3,13	-	RW+WN	12,90	1,81
25	BOMJ	FL+WN	3,20	-	FL+WN	3,56	-	FL+WN	9,59	-
26	BRAZ	RW+WN	6,77	0,57	FL+WN	3,25	-	RW+WN	17,58	1,64
27	BRFT	FL+WN	3,08	-	FL+WN	3,43	-	PF+WN	5,43	-
28	CEEU	RW+WN	6,33	0,66	FL+WN	3,52	-	FL+WN	8,06	0,28
29	CEFE	FL+WN	3,72	-	FL+WN	3,82	-	FL+WN	9,76	0,33
30	CEFT	RW+WN	8,03	0,48	FL+WN	3,34	-	FL+WN	7,45	-
31	CESB	RW+WN	4,95	0,36	FL+WN	2,63	-	FL+WN	6,35	-

[1] The symbol "-" indicates that the estimation made did not obtain a noise value for the specified model.

Table A: Noise variances and selected stochastic models of GPS sites

Continue

ORD	SITE	EAST			NORTH			UP		
		MODEL	σ_{PL} (mm/yr$^{-k/4}$)	σ_{WN} (mm)	MODEL	σ_{PL} (mm/yr$^{-k/4}$)	σ_{WN} (mm)	MODEL	σ_{PL} (mm/yr$^{-k/4}$)	σ_{WN} (mm)
32	CHPI	FL+WN	2,86	-	FL+WN	3,32	-	FL+WN	7,75	0,40
33	COAM	FL+WN	2,10	0,14	FL+WN	2,46	0,09	RW+WN	14,39	0,99
34	CORU	WN	-	0,15	PF+WN	0,11	-	WN	-	1,47
35	CRAT	RW+WN	8,60	0,76	FL+WN	3,75	-	FL+WN	11,15	-
36	CRUZ	FL+WN	2,35	0,31	FL+WN	2,82	-	FL+WN	7,52	-
37	CUIB	RW+WN	6,05	0,74	RW+WN	5,88	0,87	FL+WN	10,02	0,64
38	EESC	RW+WN	5,39	0,48	FL+WN	2,84	-	FL+WN	6,95	-
39	GOGY	FL+WN	2,50	-	FL+WN	2,84	-	FL+WN	7,83	-
40	GOJA	FL+WN	3,41	0,24	FL+WN	3,97	-	FL+WN	8,97	1,41
41	GOUR	FL+WN	2,10	-	FL+WN	2,49	-	FL+WN	6,99	-
42	GVA1	FL+WN	2,46	-	FL+WN	2,58	-	FL+WN	7,59	-
43	GVAL	FL+WN	3,10	0,69	FL+WN	3,99	0,46	FL+WN	10,96	2,12
44	IFSC	FL+WN	2,69	-	FL+WN	2,56	0,38	FL+WN	8,75	0,51
45	ILHA	FL+WN	3,38	-	FL+WN	3,24	-	FL+WN	8,49	1,43
46	IMBT	FL+WN	3,09	-	FL+WN	3,69	-	FL+WN	7,60	2,02
47	IMPZ	FL+WN	3,02	-	FL+WN	3,63	-	FL+WN	7,96	-
48	ITAI	WN	-	0,42	PF+WN	0,12	0,01	PF+WN	1,01	0,03
49	ITAM	FL+WN	1,77	0,45	FL+WN	1,63	0,60	RW+WN	17,39	1,21
50	JAMG	FL+WN	1,71	0,27	WN	-	0,90	WN	-	2,80
51	MABA	FL+WN	3,07	-	FL+WN	3,34	-	FL+WN	8,81	-
52	MABB	RW+WN	5,36	0,41	FL+WN	2,61	-	FL+WN	6,98	-
53	MABS	FL+WN	3,33	0,35	FL+WN	3,03	-	FL+WN	10,63	-
54	MAPA	FL+WN	4,27	-	FL+WN	3,77	0,86	FL+WN	7,80	1,46
55	MCL1	FL+WN	2,78	-	FL+WN	2,50	-	FL+WN	7,11	-
56	MCLA	FL+WN	3,62	0,45	FL+WN	3,67	0,12	FL+WN	10,11	-
57	MGBH	FL+WN	3,31	-	FL+WN	3,58	-	FL+WN	9,48	-
58	MGIN	FL+WN	3,41	-	FL+WN	3,43	-	FL+WN	8,21	-
59	MGMC	FL+WN	3,22	-	FL+WN	3,65	-	FL+WN	8,42	-
60	MGMT	WN	-	0,38	PF+WN	0,13	-	PF+WN	0,38	0,01
61	MGRP	FL+WN	2,92	-	FL+WN	3,45	-	FL+WN	8,50	-
62	MGUB	FL+WN	2,97	-	FL+WN	3,68	-	FL+WN	9,61	-
63	MGV1	FL+WN	2,53	-	FL+WN	2,86	-	FL+WN	7,21	-
64	MGVA	FL+WN	2,68	0,46	FL+WN	4,04	-	FL+WN	10,46	-
65	MSAQ	WN	-	0,88	WN	-	0,81	WN	-	2,73
66	MSCB	WN	-	0,38	WN	-	0,31	WN	-	1,42
67	MSCG	FL+WN	3,62	0,76	FL+WN	4,19	0,72	FL+WN	10,68	1,14
68	MSCO	FL+WN	2,31	-	WN	-	0,99	FL+WN	6,98	0,61

Table A: Noise variances and selected stochastic models of GPS sites

Continue

ORD	SITE	EAST			NORTH			UP		
		MODEL	σ_{PL} (mm/yr$^{-k/4}$)	σ_{WN} (mm)	MODEL	σ_{PL} (mm/yr$^{-k/4}$)	σ_{WN} (mm)	MODEL	σ_{PL} (mm/yr$^{-k/4}$)	σ_{WN} (mm)
69	MSDO	WN	-	1,13	WN	-	1,07	WN	-	3,14
70	MSDR	FL+WN	2,43	-	FL+WN	2,87	-	FL+WN	8,12	-
71	MSNV	PF+WN	0,09	-	WN	-	0,14	PF+WN	0,45	0,01
72	MSPP	WN	-	0,25	PF+WN	0,16	-	WN	-	1,25
73	MTBA	FL+WN	3,16	0,38	FL+WN	3,48	-	FL+WN	8,71	0,83
74	MTCN	FL+WN	2,68	-	FL+WN	2,92	-	FL+WN	7,83	-
75	MTCO	FL+WN	2,78	-	FL+WN	3,31	-	RW+WN	12,17	1,72
76	MTGA	WN	-	0,40	PF+WN	0,13	-	WN	-	1,90
77	MTJI	FL+WN	2,20	0,29	FL+WN	2,32	-	FL+WN	7,39	-
78	MTLA	PF+WN	0,14	-	WN	-	0,35	WN	-	1,40
79	MTLE	PF+WN	0,12	-	PF+WN	0,14	0,01	WN	-	1,03
80	MTNX	WN	-	0,54	FL+WN	2,28	-	FL+WN	5,74	-
81	MTSF	FL+WN	2,79	0,32	FL+WN	2,62	0,59	FL+WN	9,26	0,66
82	MTSR	FL+WN	2,65	-	FL+WN	2,79	-	FL+WN	9,30	-
83	MTVB	FL+WN	2,97	-	FL+WN	2,54	0,63	FL+WN	8,84	1,28
84	NAUS	RW+WN	5,18	0,68	FL+WN	3,43	-	RW+WN	20,75	1,60
85	NEIA	FL+WN	3,05	-	FL+WN	3,21	0,47	FL+WN	7,62	2,30
86	ONRJ	FL+WN	3,29	-	FL+WN	3,72	-	FL+WN	7,92	1,47
87	OURI	FL+WN	2,86	-	FL+WN	3,14	-	FL+WN	7,81	-
88	PAAR	WN	-	0,41	WN	-	0,52	WN	-	0,87
89	PAAT	FL+WN	2,70	-	FL+WN	3,10	-	FL+WN	9,97	-
90	PAIT	FL+WN	2,50	-	FL+WN	3,49	-	FL+WN	8,94	-
91	PARA	WN	-	0,83	PF+WN	0,20	-	WN	-	2,47
92	PASM	FL+WN	2,16	0,33	FL+WN	2,12	0,28	RW+WN	12,50	1,59
93	PAST	FL+WN	2,85	-	FL+WN	3,02	-	FL+WN	14,52	-
94	PBCG	RW+WN	5,88	0,68	FL+WN	3,51	-	FL+WN	8,16	-
95	PBJP	FL+WN	3,33	-	FL+WN	4,18	-	FL+WN	6,60	1,26
96	PEAF	FL+WN	2,99	-	FL+WN	2,48	0,21	FL+WN	7,67	-
97	PEPE	RW+WN	5,66	0,70	FL+WN	3,39	-	FL+WN	8,42	-
98	PICR	RW+WN	5,47	0,35	FL+WN	2,49	-	FL+WN	8,38	-
99	PIFL	FL+WN	2,61	-	FL+WN	2,22	0,41	FL+WN	7,11	-
100	PISR	RW+WN	5,34	0,62	FL+WN	3,70	-	FL+WN	8,50	-
101	PITN	FL+WN	2,78	-	FL+WN	2,92	-	FL+WN	7,20	-
102	POAL	FL+WN	3,09	-	FL+WN	3,64	-	PF+WN	7,08	0,01
103	POLI	FL+WN	3,70	-	FL+WN	4,72	-	FL+WN	9,48	-
104	POVE	FL+WN	2,80	0,30	FL+WN	3,77	0,41	FL+WN	7,72	-
105	PPTE	FL+WN	2,79	0,14	FL+WN	3,21	-	FL+WN	7,91	-

Table A: Noise variances and selected stochastic models of GPS sites

Continue

ORD	SITE	EAST			NORTH			UP		
		MODEL	σ_{PL} (mm/yr$^{-k/4}$)	σ_{WN} (mm)	MODEL	σ_{PL} (mm/yr$^{-k/4}$)	σ_{WN} (mm)	MODEL	σ_{PL} (mm/yr$^{-k/4}$)	σ_{WN} (mm)
106	PRCV	FL+WN	2,78	-	FL+WN	3,41	-	FL+WN	6,76	1,05
107	PRGU	RW+WN	5,70	0,68	FL+WN	3,42	-	FL+WN	9,00	-
108	PRMA	FL+WN	3,00	-	FL+WN	3,40	-	FL+WN	8,19	0,41
109	RECF	FL+WN	3,54	-	RW+WN	5,66	1,03	FL+WN	7,12	1,63
110	RIOB	FL+WN	2,66	-	FL+WN	3,03	0,40	FL+WN	7,48	1,09
111	RIOD	FL+WN	3,39	-	FL+WN	3,79	-	FL+WN	9,40	-
112	RJCG	FL+WN	3,53	-	FL+WN	3,56	-	FL+WN	8,05	-
113	RNMO	RW+WN	6,25	0,67	FL+WN	4,26	-	FL+WN	8,60	0,99
114	RNNA	RW+WN	5,92	0,81	FL+WN	3,82	-	FL+WN	8,56	0,46
115	RNPF	RW+WN	4,93	0,39	FL+WN	2,64	0,02	FL+WN	7,66	-
116	ROCD	FL+WN	3,32	-	FL+WN	3,48	-	FL+WN	8,22	-
117	ROGM	FL+WN	2,74	0,23	FL+WN	3,60	0,39	RW+WN	14,20	2,35
118	ROJI	FL+WN	2,70	0,35	FL+WN	3,58	-	FL+WN	8,13	1,01
119	ROSA	FL+WN	2,58	0,61	FL+WN	3,84	0,08	FL+WN	8,32	-
120	RSAL	RW+WN	4,59	0,48	RW+WN	4,68	0,73	FL+WN	7,01	1,94
121	RSCL	FL+WN	3,30	-	FL+WN	2,81	-	FL+WN	8,02	0,99
122	RSPE	RW+WN	4,99	0,47	FL+WN	2,97	-	FL+WN	8,26	0,86
123	RSPF	PF+WN	0,07	-	PF+WN	0,12	-	WN	-	1,70
124	SAGA	FL+WN	2,58	0,42	RW+WN	4,78	0,79	RW+WN	14,16	2,58
125	SALU	RW+WN	4,58	0,67	FL+WN	3,38	-	FL+WN	8,00	-
126	SALV	WN	-	1,12	WN	-	1,01	WN	-	3,18
127	SAVO	FL+WN	3,44	0,32	FL+WN	3,69	-	PF+WN	8,21	-
128	SCAQ	RW+WN	6,30	0,42	RW+WN	5,74	0,49	FL+WN	8,45	-
129	SCCH	FL+WN	4,02	0,78	FL+WN	3,77	-	FL+WN	8,99	1,21
130	SCFL	FL+WN	3,30	-	FL+WN	2,67	-	FL+WN	6,92	1,31
131	SCLA	FL+WN	2,66	-	FL+WN	3,13	-	FL+WN	8,94	-
132	SEAJ	FL+WN	2,86	-	FL+WN	3,21	-	FL+WN	8,19	1,02
133	SJRP	FL+WN	2,95	-	FL+WN	3,39	-	FL+WN	7,94	0,77
134	SJSP	RW+WN	5,84	0,37	RW+WN	5,59	0,41	FL+WN	6,42	-
135	SMAR	FL+WN	3,13	-	FL+WN	3,83	-	FL+WN	9,95	1,00
136	SPAR	FL+WN	2,82	-	FL+WN	3,31	-	FL+WN	7,57	-
137	SPBO	FL+WN	3,26	-	FL+WN	2,74	-	FL+WN	8,46	2,93
138	SPBP	WN	-	0,93	WN	-	0,78	WN	-	2,07
139	SPC1	FL+WN	2,25	-	FL+WN	2,39	-	FL+WN	6,88	-
140	SPCA	FL+WN	2,39	0,48	FL+WN	3,58	-	FL+WN	7,61	-
141	SPDR	FL+WN	2,45	-	FL+WN	2,47	-	RW+WN	12,72	1,89
142	SPFE	FL+WN	1,74	-	WN	-	0,86	FL+WN	5,80	0,50

Table A: Noise variances and selected stochastic models of GPS sites

Continue

ORD	SITE	EAST			NORTH			UP		
		MODEL	σ_{PL} (mm/yr$^{-k/4}$)	σ_{WN} (mm)	MODEL	σ_{PL} (mm/yr$^{-k/4}$)	σ_{WN} (mm)	MODEL	σ_{PL} (mm/yr$^{-k/4}$)	σ_{WN} (mm)
143	SPFR	FL+WN	1,76	0,39	FL+WN	2,53	-	FL+WN	7,11	-
144	SPJA	FL+WN	2,62	-	FL+WN	3,22	-	FL+WN	6,74	-
145	SPLI	FL+WN	2,64	-	FL+WN	2,72	-	FL+WN	7,21	-
146	SPPI	FL+WN	2,28	-	FL+WN	2,43	-	FL+WN	7,17	-
147	SPS1	FL+WN	2,36	-	FL+WN	2,41	-	FL+WN	5,24	0,84
148	SPSO	FL+WN	2,47	-	FL+WN	2,69	-	WN	-	2,80
149	SPTU	FL+WN	2,43	-	FL+WN	2,34	-	RW+WN	10,50	1,82
150	SSA1	RW+WN	6,12	0,91	FL+WN	3,80	-	FL+WN	9,70	-
151	TOGU	FL+WN	3,02	-	FL+WN	3,51	-	FL+WN	9,19	-
152	TOPL	FL+WN	3,10	-	FL+WN	3,43	-	FL+WN	9,16	-
153	UBA1	RW+WN	7,21	0,80	RW+WN	7,85	0,82	FL+WN	8,66	1,18
154	UBAT	WN	-	1,10	WN	-	1,27	WN	-	4,03
155	UBE1	FL+WN	2,60	-	FL+WN	2,61	-	FL+WN	8,06	-
156	UBER	WN	-	1,16	FL+WN	3,64	0,69	FL+WN	9,72	0,47
157	UFPR	FL+WN	2,84	-	FL+WN	3,60	-	FL+WN	7,60	-
158	VARG	RW+WN	7,63	0,82	FL+WN	4,13	-	FL+WN	6,95	1,63
159	VICO	FL+WN	3,51	-	FL+WN	4,10	-	FL+WN	8,84	-

* WN: White noise; FL: Flicker noise; RW: Random-walk; PF: Power-Law (fractional) noise; PL: Power-Law noise